

The Influence of Thermistor Location on Temperature Measurement from a Photonic Package

Cormac Eason¹, Marc Rensing¹, Jun Su Lee¹, Peter O'Brien¹

¹Photonics Packaging Group,
Tyndall National Institute,
Prospect Row,
Cork City,
IRELAND

cormac.eason@tyndall.ie

This paper begins by describing some commonly used photonic packages. The requirements for optical connections to these packages are then discussed. Photonic packages are different to most electronic packages in that the thermal management requirements usually include maintaining the Photonic Integrated Circuit (PIC) at a fixed, sometimes below ambient, operating temperature rather than with keeping the temperature of a package below an upper limit as with most electronic packages. This means that an active Thermoelectric Module (TEM) based cooling system is required. A thermistor is fitted within the package to provide thermal feedback to the TEM controller. This paper uses finite element modelling to investigate whether there is a good match between the target temperature for the PIC and the temperature registered by the thermistor. The results of the modelling show that the model results are quite stable even with large variations in convection and thermistor thermal properties. The thermistor location influences the temperature measured from the package and its thermal response time, but follows the device temperature well enough to provide the TEM controller with adequate feedback to maintain the PIC at a steady temperature in steady state running conditions.

1. Photonic package types

Photonic packages, similarly to electronic packages, allow the required electrical connections to be made to the Photonic Integrated Circuit (PIC) for transfer of data, powering of the Thermoelectric Module (TEM) and temperature monitoring of the PIC. This is usually accomplished using pins built into the package and insulated from the package case. Wire bonds in gold wire are used to make the connections from the PIC to the package pins.

Combined with the electrical requirements, photonics packages must also provide a means by which light can enter and/or leave the package. Directing the light into or from the package using optical fibres is the most common method. The fibres are either welded or glued in place usually after submicron alignment with the PIC to ensure high coupling efficiency. Where light detectors are required for light sources not coupled to a fibre, a window or lens is integrated within the package case to allow light in and out of the package.

It is for this reason that kovar, an iron alloy with a low thermal expansion coefficient, is used heavily in photonics packaging. A kovar package can be fitted with a glass, quartz or sapphire window/lens with minimal thermal stress between the window and package case material. This allows



reliable hermetically sealed photonic packages to be created. Kovar's poor thermal conductivity ($\approx 17 \text{ W/mK}$) does mean there is a thermal cost to using this material.

1.1. 14 Pin butterfly package

One of the most common photonic packages is known as a butterfly package. There are a number of varieties in this package, but the most common is a 14 pin package with a tube through one of the short walls to allow an optical fibre to be fed into the package. A metal lid can be resistance welded over the open top of the package allowing it to be hermetically sealed. The package footprint dimensions are $30 \text{ mm} \times 12.7 \text{ mm} \times 7.8 \text{ mm}$.

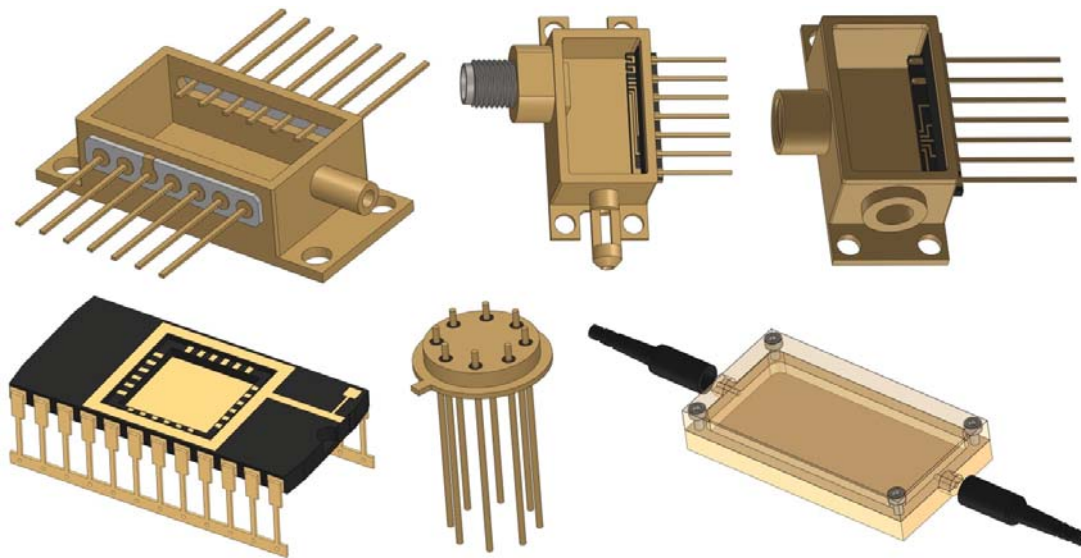


Figure 1. Starting at top left and going clockwise: 14 Pin butterfly Package, 7 Pin SMA package, 7 Pin V-Connector package, custom clamshell package, TO Package, DIL Package.

Images are not to scale with each other.

1.2. Butterfly package with high speed connection

This package looks similar to the 14 pin package and matches its dimensions closely, but loses the 7 pins from one side to allow a high speed SMA, V or GPPO (Not shown) connector in the package instead. These connectors can handle signal frequencies in the GHz range. These are required where high speed electrical signals must be converted to or from an optical signal.

1.3. Clamshell package

These packages are generally completely custom made and consist of two nearly identical halves which are bolted together to close the package. These are used when the optical coupling and electrical connection requirements or the size requirements of certain devices prevent them from fitting in off the shelf packages. The dimensions of the package shown are $49 \text{ mm} \times 26 \text{ mm} \times 9.1 \text{ mm}$.

1.4. Transistor Outline (TO) package

These are small mass produced packages, usually used where lower cost or smaller size is important. Lids are available for these packages with various lenses and windows to allow light to access the package. Many mass produced lasers and photodiodes are packaged in TOs. The TO shown in Figure 1 is 4.6 mm in diameter and the pins through it are 15.4 mm long but bigger and smaller TO packages are available.

1.5. Dual In-Line (DIL) package

These are rectangular packages commonly used in the electronics industry with a row of electrical pins along each of the long sides of the package. These can be adapted for photonics use. The DIL shown in Figure 1 is 30.5 mm × 15.6 mm × 9.2 mm in size.

2. Optical coupling to photonic devices

Indium Phosphide (InP) PICs can be used to make lasers and optical detectors. In order to couple light to and from these PICs, the fibre must be aligned with a waveguide in the top surface of the PIC. The fibre axis lies in the same plane as the PIC surface. In most cases the fibre is aligned and held in place using a nickel clip, which is laser welded to a stepped kovar submount that also carries the PIC. This is shown in Figure 2. A photograph of the laser welded fibre and a small laser is shown in Figure 3.

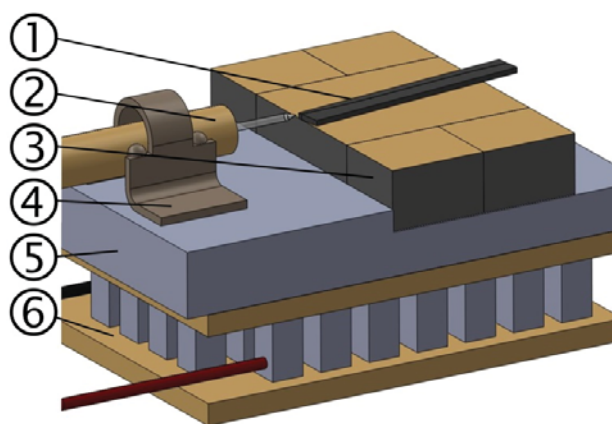


Figure 2. Fibre coupling to edge of PIC. (1) Indium Phosphide (InP) PIC, (2) Optical fibre, (3) AlN Submount, (4) Weld Clip (Nickel) laser welded to fibre and submount, (5) Kovar submount, (6) TEM.

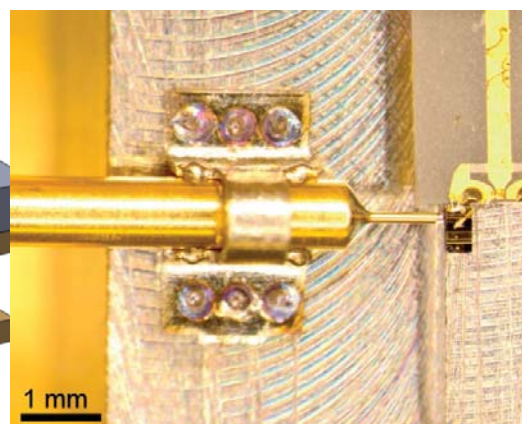


Figure 3. Photograph of laser welded fibre. Laser shown is much smaller than the one modelled in this work. The optical fibre diameter at the weld clip is 0.9 mm

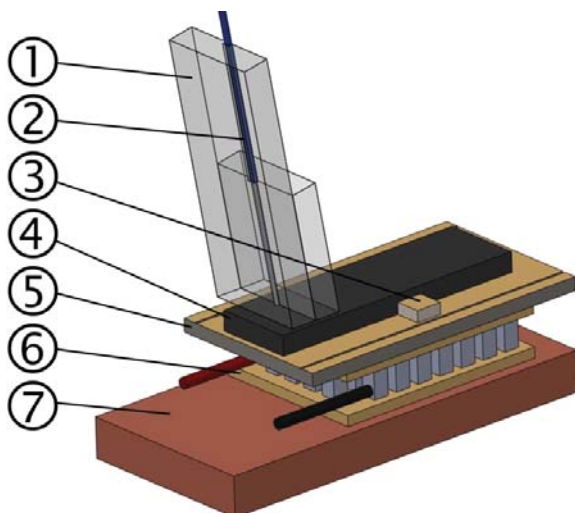


Figure 4. SOI fibre coupling using angled glass block carrying the optical fibre. The block is held in place using UV curing adhesive once it has been aligned. The assembly consists of; (1) Glass Block, (2) Optical fibre, (3) Thermistor, (4) Silicon on Insulator PIC, (5) AlN submount, (6) TEM, (7) Copper heat spreader used to spread the waste heat from the TEM before it reaches the kovar wall of the butterfly package.

Silicon on Insulator (SOI) PICs are a more recent development^[1] and allow manufacturing techniques already proven with silicon integrated circuits, to be also be applied to PIC manufacture.

These devices consist of single crystal silicon wafers with an insulating layer of usually silicon dioxide onto which a further much thinner layer of silicon or other materials is deposited. To couple light to these devices, the light must hit a grating on the PIC surface at the correct angle of incidence (Often in the region of 10° from the vertical). To accomplish this, the fibre is usually placed in a glass block polished to the required angle, which is aligned and glued to the grating on the surface of the PIC. This is shown in Figure 4.

Many other materials are used in PICs in small amounts. These materials are engineered to produce or respond to light of various colours based on the band gap of the material. In many cases these materials are used in submicron thick layers on a substrate of silicon or InP. The thermal behaviour of these layers makes very little difference to the bulk temperature of the PIC. Gradients or localised hot spots may measurably alter optical behaviour however.

3. Thermal management

Photonic devices in most cases have low power requirements and as such their thermal management tends to be less demanding than more powerful electronic devices. The difference however is that the optical properties of photonic devices change with temperature, leading to undesirable device behaviour even though the package never overheats.

For this reason most packages are temperature regulated using TEMs rather than just cooled. The operation of these devices adds further waste heat to the package, but this is within ranges that can be dealt with using off the shelf heat sinking even while using mostly kovar packages.

The main uncertainty in most packages is whether the temperature read from the thermistor matches with the temperature experienced by the working parts of the PIC. This will be investigated for the package shown in Figure 5. The package consists of a butterfly package holding a laser. The temperature of the laser is regulated using a TEM and an optical fibre is welded in alignment with the emitting edge of the laser. The laser sits on a metallised Aluminium Nitride (AlN) submount, and wirebonds to connect the laser and thermistor to the package pins. The thermistor is mounted on the top right of the metallised AlN submount.

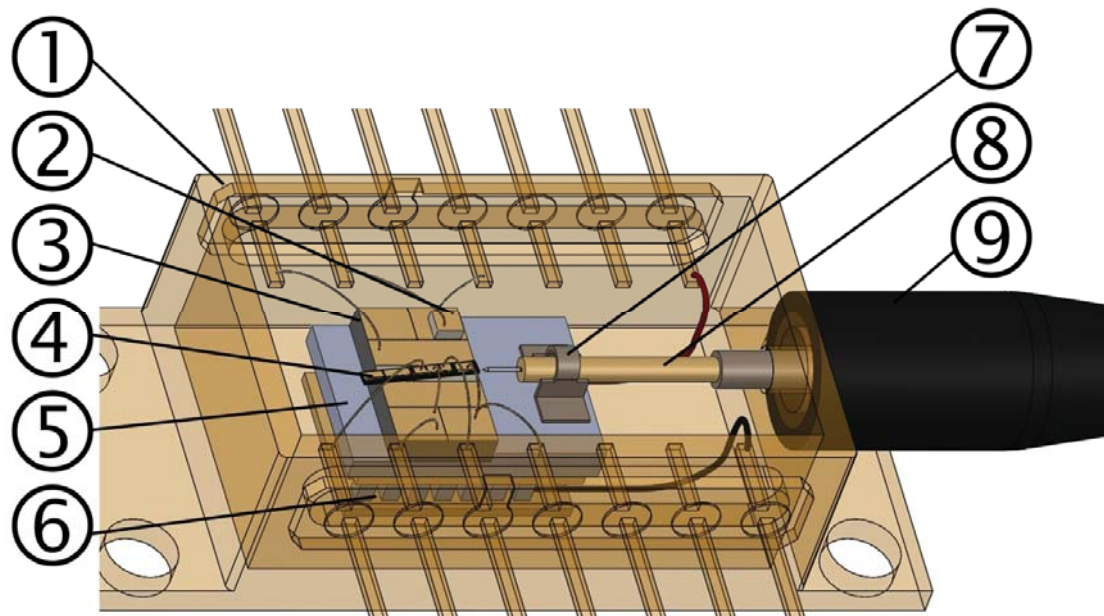


Figure 5. The assembly from which the geometry used to build the finite element model was sourced. Assembly consists of; (1) Kovar butterfly package, (2) Thermistor, (3) AlN submount, (4) Laser, (5) Kovar submount, (6) TEM, (7) Weld clip, (8) Fibre, (9) Fibre strain relief.

The location of the thermistor is clearly less than optimal to measure the PIC temperature but in order to provide a ground electrical connection to the thermistor using one of the metallised islands on the AlN submount, it was necessary to move it away from the laser. This sort of compromise is common in photonic packages, especially in the case of prototypes, as the supporting electrical and optical connections for the PIC are more critical than placing the thermistor in an ideal location.

In terms of relative sizes, the laser in this model is 4.3 mm long, less than 5 μm wide and deep and on a die 0.5 mm wide and 0.1 mm thick while the thermistor is 0.6 mm \times 0.6 mm \times 0.3 mm in size, which means the thermistor has just under half the total volume of the PIC. Thermistors small enough to match the scale of the features on the PIC are not to the authors' knowledge available. Finding an ohmmeter with a low enough driving current/voltage to prevent the thermistor from self heating and affecting its own resistance and creating a further hot spot within the package is likely to prove difficult at this scale also.

Mounting the thermistor directly to the PIC is avoided as mechanical bonding to the PIC surface can lead to mechanical or thermal strain and the potential malfunction of the waveguides and other components on the PIC^[2].

In this package the AlN PIC submount is carried on a further submount, to which the weld clip that holds the fibre is also attached. The submount is made from kovar as this is compatible with the laser welding process. The clip holding the fibre is made from nickel. The thickness of the submount is varied to center the fibre vertically with the surface of the PIC and with the hole in the butterfly package wall through which the fibre enters.

4. Finite element model

A finite element model of the laser package was created in COMSOL Multiphysics to examine the correlation between the temperature measured by the thermistor and the temperature of the laser.

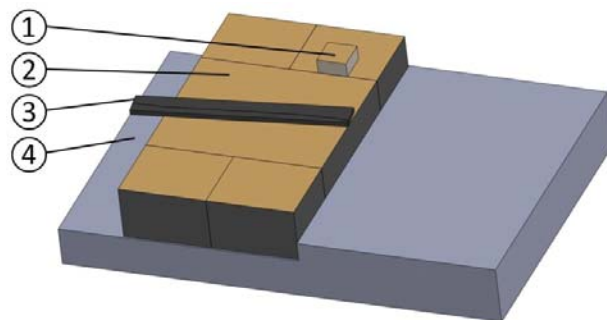


Figure 6. CAD Geometry for Models M1-M7 and M9. (1) Thermistor, (2) Metallised Aluminium Nitride (AlN) submount, (3) Laser (InP), (4) Kovar submount.

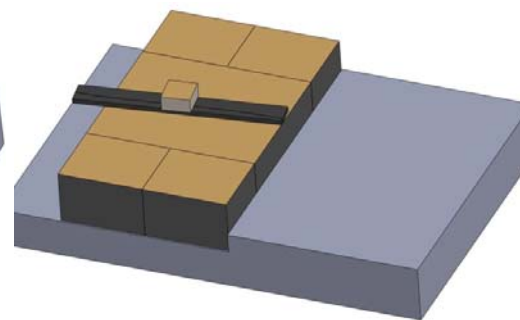


Figure 7. CAD geometry for Models M8 and M10. Thermistor has been placed on top of the laser. This configuration would not be used in a working device.

The stepped submount is made from Kovar, the metallised submount is made from AlN and the laser PIC is made from InP. Neither the thermistor material or its thermal properties are given on the manufacturer's data sheet. For the purposes of the analysis it has been given the properties of Alumina. Models are run to investigate the sensitivity of the results to the thermal conductivity of the thermistor to see whether this measurement is critical.

The laser is modelled as a line heat source of 0.3 W total power. The CAD model of the PIC carrying the laser is split vertically along the path of the laser and the top edge of the split is used as a line heat source representing the laser. Since the cross sections of InP based lasers are typically less than 5 μm \times 5 μm and the laser is 4.3 mm long, the laser has an aspect ratio in the region of 1000:1.

Massive numbers of elements would be required to fill this volume with the low aspect ratio elements required for good convergence if a solid model of the laser was used.

All parts of the assembly are glued together using a high silver content thermally and electrically conductive epoxy from Epoxy Technology Inc. (EPO-TEK H20E). The bond line thickness is generally 50 μm. This is modelled as 50 μm thick thermally resistive layer of conductivity 2.5 W/mK at the interface between each component in the assembly.

The cooling provided by the TEM is modelled as a constant temperature of 20°C applied to the underside of the kovar submount while all the other boundary surfaces of the model had a natural convection boundary condition applied based on Equation 1^[3]. It should be noted that the convection coefficient is not the same for all surfaces in reality and that the experimental measurement of natural convection heat transfer from such small areas on a working photonic package presents significant practical difficulties. To account for this, models were run with no convection and with an order of magnitude more convection than the chosen value to investigate the sensitivity of the model to this uncertainty.

$$h = \frac{k}{L} \left(0.68 + \frac{0.67 Ra_L^{1/4}}{(1 + (0.492/Pr)^{9/16})^{4/9}} \right)$$

Equation 1

h = Convection Coefficient (W/m ² K)	$h \approx 27$ W/m ² K
k = Thermal Conductivity of air (W/mK)	$k \approx 0.026$ @ 20°C
L = Characteristic Length of surface of interest (m)	$L \approx 0.001$ m
Pr = Prandtl number (No unit) = ν/α	$Pr \approx 0.716$
Gr_L = Grashof number (No unit) = $g\beta(T_s - T_\infty)L^3\nu^{-2}$	$Gr_L \approx 0.733$
Ra_L = Rayleigh number (No unit) = $Gr_L \times Pr$	$Ra_L \approx 0.052$
g = gravitational acceleration (m/s ²), β = volumetric thermal expansion coefficient (1/K), T_s = temperature of convecting surface (K), T_∞ = temperature of ambient air (K), ν = kinematic viscosity (m ² /s)	

The nominal value of 26 W/m²K found based on this is high for a natural convection coefficient, but arises as a consequence of the small characteristic dimensions of the convecting surfaces. The results from model M2 show that the TEM provides the dominant heat path from the device, making the exact determination of the convection coefficient unimportant in the overall process of predicting the final temperature of the device.

4.1. Grid independence check

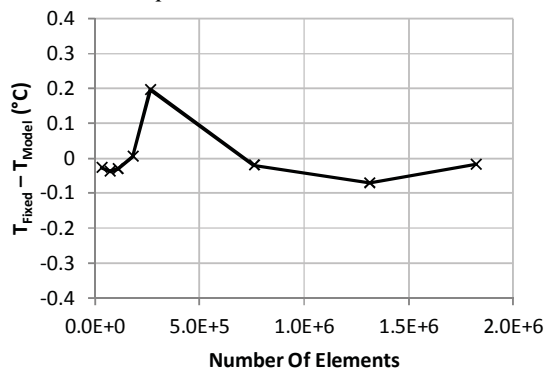


Figure 8. Grid independence check on model. T_{Fixed} is the average of the maximum temperatures measured from each model.

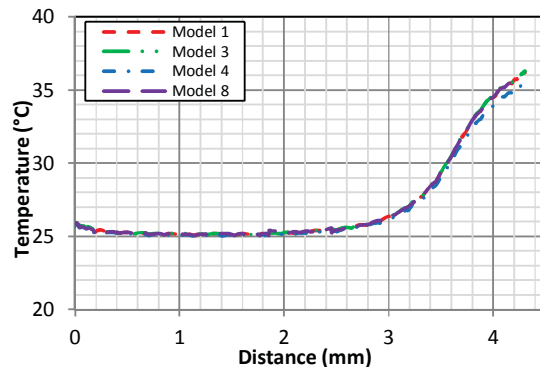


Figure 9. Temperature profile along the laser for various models run. Note high temperature in the laser where it does not contact the submount.

Seven models were run at varying mesh densities from 32 619 to 1 822 326 elements. The largest variation in the temperature results was found to be under $\pm 0.2^\circ\text{C}$ of the average temperature across all the models, with most results being well within 0.1°C of the average as can be seen in Figure 8. This gave good confidence that the 32 619 element model used for the analysis would give acceptably accurate results.

5. Models run and results:

A list of the models run in this study is given in Table 1. The baseline model against which the other models are compared is model M1 (Geometry shown in Figure 10). This uses the best estimates for values of the convection coefficient and the thermistor conductivity. Model M2 was run without modelling the effect of the TEM in maintaining the temperature of the device. It can be seen from this that without the TEM the device runs over 100°C hotter, indicating that the natural convection heat transfer is not the dominant means by which the temperature of the device is maintained.

Table 1. List of finite element models run in this study.

Model	h (W/m ² K)	k_{Th} (W/mK)	T_{Max} (°C)	T_{AvgTh} (°C)	T_{AvgL} (°C)	$T_{AvgL} - T_{AvgTh}$
M1	26	27	36.22	20.74	27.12	6.38
M2 (TEM Off)	26	27	144.98	129.88	136.33	6.45
M3	0	27	36.29	20.75	27.14	6.39
M4	260	27	35.55	20.70	26.94	6.24
M5	26	2.7	36.22	20.74	27.12	6.38
M6	26	270	36.22	20.74	27.12	6.38
M7	260	270	35.55	20.70	26.94	6.24
M8 (Thermistor on Laser)	26	27	36.21	25.23	27.12	1.89
M9 (M1 Transient @ 10s)	26	27	36.23	20.75	27.14	6.39
M10 (M8 Transient @ 10s)	26	27	36.21	25.35	27.12	1.77

To further investigate the influence of the convection coefficient on the device temperatures, model M3 was run with no convection heat loss at all. This increased the average temperature of the laser by 0.02°C . Similarly when the convection coefficient was increased by an order of magnitude as in model M4, the laser temperature dropped by 0.18°C . This confirms that the TEM cooling effect is the dominant influence on the laser temperature.

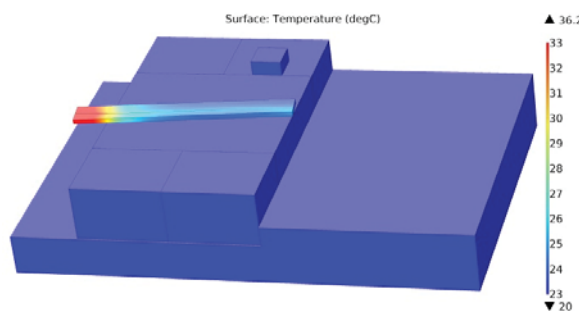


Figure 10. Temperature results from M1.

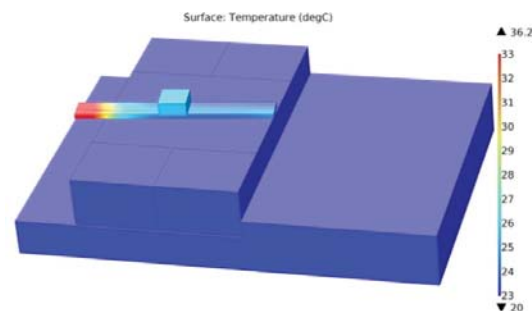


Figure 11. Temperature results from M8.

Models M5 and M6 then looked at the effect of the properties of the thermistor on the temperature it measures. No properties for the thermistor material were available as neither the material nor any of its properties apart from its resistance-temperature characteristics were included on the datasheet. The result from models M5 and M6 shows that a drop or a gain of an order of magnitude in the

thermistor's thermal conductivity has no influence on the average temperature of the thermistor to two decimal places compared to the baseline model M1.

Model M7 was then run to see whether the combination of high thermal conductivity and high convection heat transfer would allow the thermistor to act as a heat sink fin and reduce its temperature. The average temperature of the thermistor in model M7 only dropped by 0.04°C from models M1, M5 and M6, indicating that the temperature indicated by the thermistor is a reliable representation of the temperature of the surface it is fitted to even with high uncertainty as to its actual properties and large variation in the convection conditions around it.

The other important result from this is that even though the thermistor in models M1-M7 does not give the correct device temperature, it does give a temperature that follows the device temperature well enough to provide decent temperature feedback to the TEM controller. Even when the model was run without the TEM cooling effect (Model M2), the difference in temperature between the thermistor and the laser shifted from 6.38°C to 6.45°C , a change of just over 1%.

Model M8 was run with the thermistor placed on the laser instead of to the side of it as in the other models. The thermistor conductivity and convection coefficient were left at the same values as model M1. The results from this model show that, as expected, having the thermistor closer to the laser gives a better temperature measurement (See Figure 11). While the thermistor is still 1.89°C below the average laser temperature it is important to note that the average temperature of the area of the laser the thermistor makes contact with is 25.35°C , or 0.12°C more than the thermistor temperature. This confirms that if it was possible to fit the thermistor directly on the laser surface without potential damage to the laser it would represent the temperature of the laser well despite the volume mismatch.

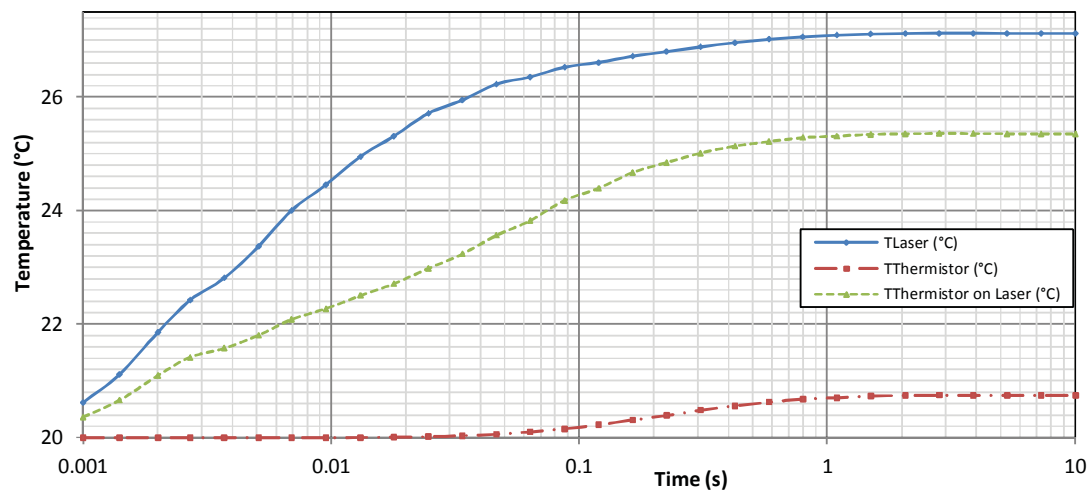


Figure 12. Transient temperature results M9 and M10. T_{Laser} is the average temperature along the line representing the laser in both models, $T_{\text{Thermistor}}$ is the average temperature of the volume representing the thermistor and $T_{\text{Thermistor on Laser}}$ is the average temperature of the thermistor for the case where the thermistor is placed on top of the laser.

Model M9 was run at the same settings as model M1 but as a transient model to see how well the thermistor follows the temperature of the laser as the laser is turned on. Thirty logarithmically spaced time steps from 0.001 s to 10 s were used in order to capture the very quick initial thermal response of the laser as well as the steady state final temperatures of the system.

While there is a noticeable delay of the order of 0.02 seconds before the thermistor responds to the laser turning on, both the laser and the thermistor reach a steady state in approximately 2 seconds. This confirms that the thermistor can be used as a representative temperature for the laser for the feedback

loop to the TEM. In the case of a laser that is switching on and off however, a much quicker temperature response would be needed.

Model M10 was run with the same time steps as model M9 but with the thermistor on the laser geometry from model M8. The time-temperature curves from models M9 and M10 are shown in Figure 12.

5.1. Further assembly issues

The section of the laser which overhangs the submount can be seen to run significantly hotter than the laser in contact with the submount in Figure 10 and Figure 11. This gave acceptable performance for the prototyping of this particular package but would not be acceptable in many cases. A plot of the temperature profile along the laser is shown in Figure 9. This is detrimentally affecting the average laser temperature and does reduce the correlation between the thermistor temperature and the laser temperature.

It can also be seen in Figure 9 that as a result of the higher convection coefficient used in model M4, the temperature of the unsupported end of the laser can be seen to be lower than in the other models as the unsupported end of the laser is the only part of the model where the cooling isn't completely dominated by the TEM.

6. Conclusions

The results show that the finite element model results are not very sensitive to variation in convection and thermistor properties. As this information is not easily measured or freely available, this is good news for the extraction of meaningful results from finite element models of these assemblies. The important conclusions are summarised in the following points:

- The convection heat transfer from the package components does not play significant part in the temperature regulation of TEM regulated photonics packages of the type analysed.
- The only location where convection was seen to influence the TEM controlled model was where the laser extended past the edge of the submount it was fitted to. A tenfold increase in the convection coefficient altered the temperature of the overhanging end of the laser by almost 1°C.
- Even though properties for the thermistor are not available, the results from the model remain almost completely unaffected by a variation of an order of magnitude each way in the thermistor's estimated thermal conductivity.
- Using a line heat source to model the laser rather than trying to mesh it as a volume massively reduces the computing requirements and solving time for the model while still giving excellent data on the overall behaviour of the package.
- The results show good correlation between the temperature of the surface the thermistor is fitted to and the average temperature of the thermistor volume.
- The thermistor does not return temperature data that matches exactly with the temperature of the photonic components in the package due to unavoidable constraints in the assembly.
- While the thermistor mounted away from the PIC does not give an exact device temperature, it does provide a suitable value to feed to the TEM controller to maintain the packaged device at a constant temperature for steady state running conditions.
- There is a significant delay in the initial thermal response of the thermistor when the laser is turned on. This delay is reduced by mounting the thermistor directly on the component to be measured but creates an unacceptable risk of damage to the optical components due to interfacial stresses between the thermistor and the PIC making this an unacceptable option for real world assembly.
- For more precise temperature control integrating a temperature sensing element directly on the PIC itself during PIC manufacture would eliminate considerable uncertainty in this regard.

References

- [1] Kopp, Christophe; Stéphane Bernabé, Badhise Ben Bakir, Jean-Marc Fedeli, Regis Orobtcouk, Franz Schrank, Henri Porte, Lars Zimmermann, and Tolga Tekin (2011). Silicon Photonic Circuits: On-CMOS Integration, Fiber Optical Coupling, and Packaging, *IEEE Journal of Selected Topics in Quantum Electronics*, vol. 17, No. 3, May/June 2011
- [2] Huang, M. and X. Yan (2003). Thermal-stress Effects on the Temperature Sensitivity of Optical Waveguides, *J. Opt. Soc. Am. B/Vol. 20*, No. 6/June 2003.
- [3] Churchill, S.W., and Chu, H. H. S. (1975). Correlating Equations for Laminar and Turbulent Free Convection from a Vertical Plate, *Int. J. Heat Mass Transfer*, 18, 1323–1329.